

See discussions, stats, and author profiles for this publication at: <https://www.researchgate.net/publication/376350988>

Steady State Kinetics for Enzymes with Multiple Binding Sites Upstream of the Catalytic Site

Article in *Symmetry* · December 2023

DOI: 10.3390/sym15122176

CITATIONS

0

READS

46

9 authors, including:



Manuel Osorio

Universidad Andrés Bello

18 PUBLICATIONS 147 CITATIONS

SEE PROFILE



Dino Salinas

21 PUBLICATIONS 41 CITATIONS

SEE PROFILE



Felipe Valenzuela-Ibaceta

Universidad Andrés Bello

7 PUBLICATIONS 3 CITATIONS

SEE PROFILE



Fernando Danilo Gonzalez-Nilo






Universidad Andrés Bello

228 PUBLICATIONS 3,738 CITATIONS

SEE PROFILE

Article

Steady State Kinetics for Enzymes with Multiple Binding Sites Upstream of the Catalytic Site

Manuel I. Osorio ^{1,2,*} , Mircea Petrache ³ , Dino G. Salinas ², Felipe Valenzuela-Ibaceta ⁴, Fernando González-Nilo ⁴, William Tiznado ⁵ , José M. Pérez-Donoso ⁴ , Denisse Bravo ¹ and Osvaldo Yáñez ^{6,*} 

- ¹ Facultad de Odontología, Universidad Andres Bello, Santiago 8370133, Chile; denisse.bravo@unab.cl
² Facultad de Medicina, Universidad Diego Portales, Santiago 8370007, Chile; dino.salinas@udp.cl
³ Facultad de Matematicas, Pontificia Universidad Católica de Chile, Avda. Vicuña Mackenna 4860, Santiago 6904441, Chile; mpetrache@mat.uc.cl
⁴ Center for Bioinformatics and Integrative Biology, Facultad de Ciencias de la Vida, Universidad Andres Bello, Santiago 8370186, Chile; fernando.gonzalez@unab.cl (F.G.-N.); jose.perez@unab.cl (J.M.P.-D.)
⁵ Computational and Theoretical Chemistry Group, Departamento de Ciencias Químicas, Facultad de Ciencias Exactas, Universidad Andres Bello, República 498, Santiago 8370251, Chile; wtiznado@unab.cl
⁶ Núcleo de Investigación en Data Science, Facultad de Ingeniería y Negocios, Universidad de las Américas, Santiago 7500000, Chile
* Correspondence: manuel.osorio@unab.cl (M.I.O.); oyanez@udla.cl (O.Y.)

Abstract: The Michaelis–Menten mechanism, which describes the binding of a substrate to an enzyme, is a simplification of the process on a molecular scale. A more detailed model should include the binding of the substrate to precatalytic binding sites (PCBSs) prior to the transition to the catalytic site. Our work shows that the incorporation of PCBSs, in steady-state conditions, generates a Michaelis–Menten-type expression, in which the kinetic parameters K_M and V_{max} adopt more complex expressions than in the model without PCBSs. The equations governing reaction kinetics can be seen as generalized symmetries, relative to time translation actions over the state space of the underlying chemical system. The study of their structure and defining parameters can be interpreted as looking for invariants associated with these time evolution actions. The expression of K_M decreases as the number of PCBSs increases, while V_{max} reaches a minimum when the first PCBSs are incorporated into the model. To evaluate the trend of the dynamic behavior of the system, numerical simulations were performed based on schemes with different numbers of PCBSs and six conditions of kinetic constants. From these simulations, with equal kinetic constants for the formation of the Substrate/PCBS complex, it is observed that K_M and V_{max} are lower than those obtained with the Michaelis–Menten model. For the model with PCBSs, the V_{max} reaches a minimum at one PCBS and that value is maintained for all of the systems evaluated. Since K_M decreases with the number of PCBSs, the catalytic efficiency increases for enzymes fitting this model. All of these observations are consistent with the general equation obtained. This study allows us to explain, on the basis of the PCBS to K_M and V_{max} ratios, the effect on enzyme parameters due to mutations far from the catalytic site, at sites involved in the first enzyme/substrate interaction. In addition, it incorporates a new mechanism of enzyme activity regulation that could be fundamental to search for new activity-modulating sites or for the design of mutants with modified enzyme parameters.

Keywords: steady-state enzyme kinetics; multi-precatalytic binding sites; numerical simulation



Citation: Osorio, M.I.; Petrache, M.; Salinas, D.G.; Valenzuela-Ibaceta, F.; González-Nilo, F.; Tiznado, W.; Pérez-Donoso, J.M.; Bravo, D.; Yáñez, O. Steady State Kinetics for Enzymes with Multiple Binding Sites Upstream of the Catalytic Site. *Symmetry* **2023**, *15*, 2176. <https://doi.org/10.3390/sym15122176>

Academic Editors: Yueping Dong, Wanbiao Ma, Yasuhiro Takeuchi and George Papageorgiou

Received: 13 October 2023
Revised: 8 November 2023
Accepted: 13 November 2023
Published: 8 December 2023



Copyright: © 2023 by the authors. Licensee MDPI, Basel, Switzerland. This article is an open access article distributed under the terms and conditions of the Creative Commons Attribution (CC BY) license (<https://creativecommons.org/licenses/by/4.0/>).

1. Introduction

Enzymes are macromolecules, polymers of amino acids, that accelerate chemical reactions by several orders of magnitude, allowing them to occur at a rate capable of sustaining life [1]. This process occurs in a small region of the enzyme called the catalytic site, which is usually located in a groove or gap with controlled access to the solvent [2]. To access the

catalytic site, the substrate must be transferred from the solvent, traveling a path that can span 20 Å, depending on the distance from the first contact [3]. As observed in simulations of the binding of 1,2,3-trichloropropane substrate to the enzyme haloalkane dehalogenase A and haloalkane dehalogenase A31, the substrate travels a 20 Å path from the solution to the catalytic site [4]. In this pathway, as shown by simulations of enzyme/ligand complex formation, in the first stage, the substrate interacts with the enzyme surface, decreasing its mobility and the number of water molecules in its hydration layer [5]. There may be different initial binding sites for the substrate on the surface of the protein, which determines its trajectory. This behavior has been observed in the binding path of the phosphate anion to the catalytic site of the phosphate-binding protein [6]. For this particular case, it is proposed that the regions near the catalytic site show charged residues that are distributed so that the substrate is directed to the catalytic site. In the same way, molecular dynamics simulations have identified previous binding sites for the enzyme Cephalosporin Acylase, an enzyme that can be used to synthesize the synthetic antibiotic Cephalosporin [7]. A similar process is observed during molecular dynamics simulations of the binding of the inhibitor Benzamide to Trypsin, identifying sites of increased binding probability [8]. The mathematical models obtained considering steady-state kinetics have focused on multisubstrate models, for different inhibitors or systems with cooperativity, but the approach of precatalytic sites (PCBSs) has not been addressed [9,10]. The mathematical models obtained, considering steady-state kinetics, have focused on multisubstrate models for different inhibitors or systems with cooperativity, but the approach for precatalytic sites (PCBS) has not been addressed. The mathematical models obtained, considering steady-state kinetics, have focused on multisubstrate models for different inhibitors or systems with cooperativity, but the approach for precatalytic sites (PCBS) has not been addressed. Models used for enzymes with mutidomains that are cooperative, such as hemoglobin, employ the Hill equation, which has a sigmoid form but uses the same PCBS scheme [11]. To describe enzyme inhibition, the same scheme is used without PCBSs in which reversible steps representing inhibitor binding are added. If the enzyme processes several substrates, a model for several kinetic schemes is available using the same MM scheme as above. For the inhibition and multisubstrate models, the steady-state kinetics generate a rectangular hyperbole plot indistinguishable from the single-substrate case without an inhibitor, with kinetic parameters that include the factors associated with the inhibitors and the different substrates. However, all of the above models use the Michaelis–Menten scheme formulated in 1913, to which major contributions have been made, including those made by Briggs and Haldane in 1925 through those made by Schnell and Maini in 2003; the contributions are described in detail in the 2019 paper [12]. It is interesting to note that several mathematical papers have dealt with reaction networks using graph and category theory (see for example [13]) and were aimed at general theoretical aspects of reaction dynamics [14]. However, in the previous references the study of the influence of kinetic constants and the application to enzymatic dynamics, remain at a more theoretical/qualitative level than the present work. It is therefore unknown how the presence of PCBSs affects the catalytic capabilities of enzymes or whether this phenomenon could be associated with any enzyme function. To address this question we moved from the simple general scheme without PCBSs or Michaelis–Menten (MM), to one with PCBSs and evaluated how the kinetic parameters are affected by the presence of an increasing number of PCBSs. The kinetic scheme that was used in general (Figure 1a) and from which, considering steady state, the MM equation ($v = \frac{V_{max} \cdot [S]}{K_m + [S]}$) is obtained, includes the concentration of substrate (s), enzyme (e), product (p) and enzyme/substrate complex (es) (a simplified notation for concentration was used). From this model, we obtain an expression for the affinity of the enzyme for the substrate or Michaelis constant ($K_M = \frac{k_2 + k_{-1}}{k_1}$) and the maximum possible activity at a given enzyme concentration ($V_{max} = k_2 * E_{Total}$). From these kinetic parameters, it is possible to calculate the catalytic efficiency $Catalytic\ efficiency = \frac{V_{max}}{K_M}$, which is an index of the selectivity of an enzyme towards a specific substrate. Thus, as V_{max} increases and K_M decreases for a given substrate, the catalytic efficiency of the enzyme increases with

respect to that substrate, resulting in increased selectivity for that substrate. Since this is a relevant index to evaluate the activity of an enzyme, this is a widely used index to evaluate the activity of an enzyme. To evaluate the relationship between the number of PCBSs and the parameters K_M and V_{max} , we worked with a kinetic model including i-PCBSs converging at the catalytic site (Figure 1b), and, under steady-state conditions, a mathematical expression for the Michaelis–Menten-type enzyme activity was derived. This dependence was evaluated by numerical simulation, using a program written in Python, which uses the Kinetics library [15–17].

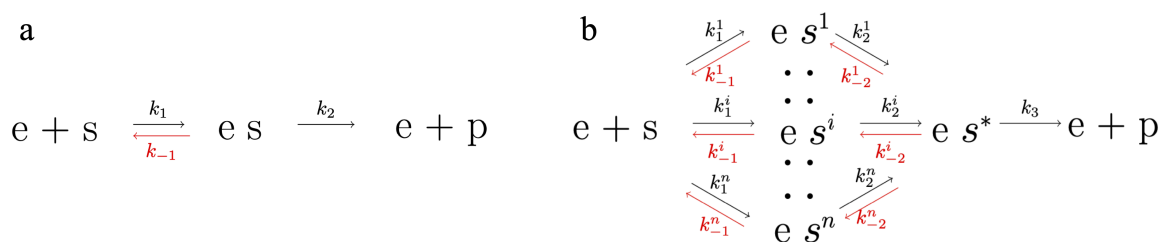


Figure 1. Kinetic schemes: (a) shows the kinetic scheme that does not consider PCBSs and (b) shows the kinetic scheme that does include PCBSs. K are kinetic constants of an elementary step with positive subscripts for steps of product formation and negative subscripts for the reverse process. For scheme (b), which includes a number n of PCBSs, the superscripts individualize each PCBS.

2. Materials and Methods

We develop in detail the mathematical framework corresponding to the reaction network from (1b) in Section 3.1, with the main simplifying hypothesis being that the system is at equilibrium, which is justified under the assumption that the substrate concentration is much larger than the enzyme concentration. To simulate kinetic systems with various PCBSs we employed the Python package Kinetics [16], which has been previously successfully used for reactions with various substrates, inhibitors and metabolic pathways for flux control analysis. In our study, we used the “generic reactions” tool of this package to obtain the kinetic parameters of systems with different numbers of PCBSs. An enzyme concentration of 0.0002 mM was used in all simulations, and initial velocities were obtained from the first 10 iterations of the simulation. Kinetic parameters were obtained for substrate concentrations of 0.1, 0.2, 0.5, 5, 10, 100 mM. All units used are referential. However, if the ratio is maintained, they can be scaled to the units used experimentally; therefore, all concentration values will be considered as mM. Equivalent PCBSs with equal binding kinetic constants k_j^i (j can take the values 1 and 2) and equal dissociation constants k_{-j}^i (j can take the values 1 and 2) were considered in the simulations. Different conditions were evaluated for the kinetic constants, but the value of the dissociation constants was kept lower than the complex formation kinetic constants $k_{-1}^i = k_{-2}^i = 0.01$, and the condition without PCBSs was simulated as a control. For all conditions evaluated, the simulation generates the parameters V_{max} and K_M , which are obtained by calculation with the constants used. For Table 1, the condition (a) $k_1^i = k_2^i > k_{cat}$ (with values of 10, 10 and 2, respectively) was considered. For Table 2, the condition (b) $k_{cat} > k_1^i = k_2^i$ (with values of 10, 2 and 2, respectively) was considered, and, for Table 3, (c) $k_{cat} > k_1^i > k_2^i$ (with values of 10, 6 and 2, respectively) was considered. For Figure 2, in addition to the conditions evaluated in the tables, three extra conditions were tested: (d) $k_{cat} > k_2^i > k_1^i$, (e) $k_1^i > k_2^i > k_{cat}$ and (f) $k_2^i > k_1^i > k_{cat}$. The Python program to simulate each condition is accessible at [16].

Table 1. Numerical simulation of enzyme kinetics for $k_2^i = k_1^i > k_{cat}$. For the simulations, the kinetic constants of substrate binding $k_1^i = 10$, dissociation constants $k_{-1}^i = 0.01$ and the catalytic constant with $k_{cat} = 2$ at an enzyme concentration of 0.0002 mM and substrate concentration of 0.1, 0.2, 0.5, 5, 10, 100 mM were used. For the analysis of kinetics, the slope of the first 10 points for each substrate concentration was taken to obtain the kinetic parameters from the reciprocal doublings.

Kinetic Parameters	Michaelis–Menten *	$i = 1$	$i = 2$	$i = 3$	$i = 4$	$i = 5$
V_{max}	4×10^{-4}	3.31×10^{-4}	3.31×10^{-4}	3.31×10^{-4}	3.330×10^{-4}	3.30×10^{-4}
K_M	20.1×10^{-2}	17.1×10^{-2}	8.64×10^{-2}	5.76×10^{-2}	4.32×10^{-2}	3.45×10^{-2}
Catalytic efficiency	19.2×10^{-4}	19.2×10^{-4}	38.3×10^{-4}	57.4×10^{-4}	76.5×10^{-4}	95.6×10^{-4}

* Numerical simulation without PCBS.

Table 2. Numerical simulation of enzyme kinetics for $k_{cat} > k_1^i = k_2^i$. For the simulations, the kinetic constants of substrate binding $k_1^i = k_2^i = 2$, dissociation constants $k_{-1}^i = 0.01$ and the catalytic constant with $k_{cat} = 10$ at an enzyme concentration of 0.0002 mM and substrate concentration of 0.1, 0.2, 0.5, 5, 10, 100 mM are used. For the analysis of kinetics, the slope of the first 10 points for each substrate concentration was taken to obtain the kinetic parameters from the reciprocal doublings.

Kinetic Parameters	Michaelis–Menten *	$i = 1$	$i = 2$	$i = 3$	$i = 4$	$i = 5$
V_{max}	2.00×10^{-3}	3.32×10^{-4}	3.32×10^{-4}	3.31×10^{-4}	3.31×10^{-4}	3.31×10^{-4}
K_M	505×10^{-2}	86.6×10^{-2}	43.3×10^{-2}	28.8×10^{-2}	21.6×10^{-2}	17.3×10^{-2}
Catalytic efficiency	3.97×10^{-4}	3.83×10^{-4}	7.67×10^{-4}	11.5×10^{-4}	15.3×10^{-4}	19.1×10^{-4}

* Numerical simulation without PCBS.

Table 3. Numerical simulation of enzyme kinetics for $k_{cat} > k_1^i > k_2^i$. For the simulations, the kinetic constants of substrate binding $k_1^i = 6$, $k_2^i = 2$, dissociation constants $k_{-1}^i = 0.01$ and the catalytic constant with $k_{cat}^i = 10$ at an enzyme concentration of 0.0002 mM and substrate concentration of 0.1, 0.2, 0.5, 5, 10, 100 mM were used. For the analysis of kinetics, the slope of the first 10 points for each substrate concentration was taken to obtain the kinetic parameters from the reciprocal doublings.

Kinetic Parameters	Michaelis–Menten *	$i = 1$	$i = 2$	$i = 3$	$i = 4$	$i = 5$
V_{max}	20.0×10^{-4}	3.32×10^{-4}	3.31×10^{-4}	3.31×10^{-4}	3.31×10^{-4}	3.31×10^{-4}
K_M	505×10^{-2}	28.9×10^{-2}	14.4×10^{-2}	9.63×10^{-2}	7.22×10^{-2}	3.46×10^{-2}
Catalytic efficiency	3.97×10^{-4}	11.5×10^{-4}	23.0×10^{-4}	34.0×10^{-4}	46.0×10^{-4}	96.6×10^{-4}

* Numerical simulation without PCBS.

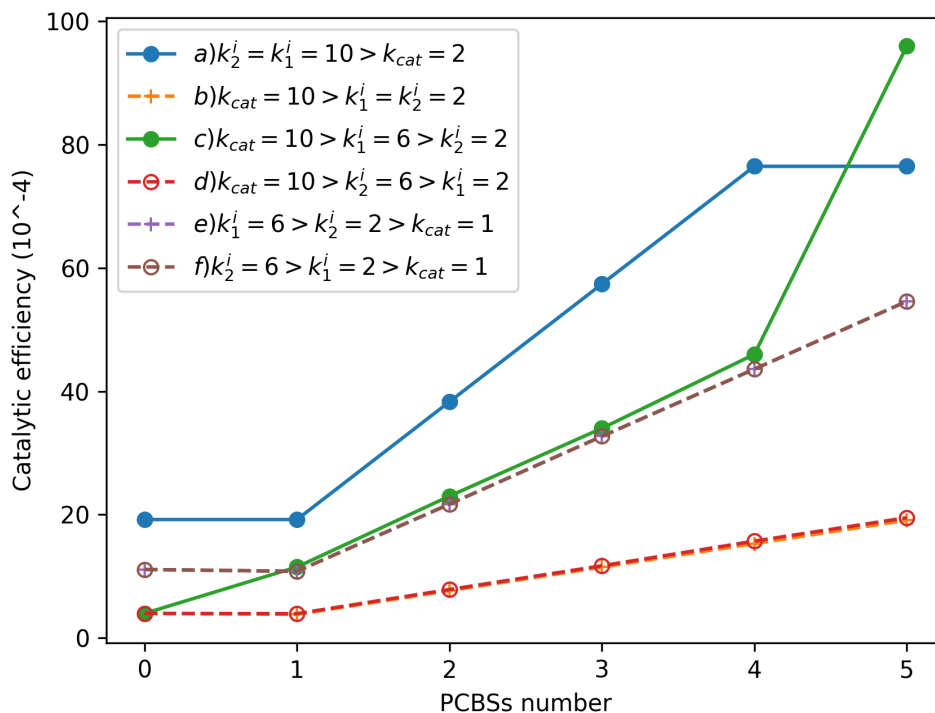


Figure 2. Increase in catalytic efficiency as a function of the number of PCBSs. Numerical simulation was performed for 6 conditions of kinetic constants for the MM model (first point $i = 0$) and with $i = 1, 2, 3, 4, 5$ and 5 PCBSs. For each simulation, the catalytic efficiency ($\frac{k_{cat}}{K_M}$) was plotted as a function of the number of PCBSs. Because curves b and d overlap, as well as e and f, these are observed with segmented lines.

3. Results

3.1. Steady-State Kinetics for an Enzyme with Several PCBSs

From scheme (1b), the species notation was changed to differentiate the free enzyme and substrate ($e + s$) from the enzyme–substrate complex (es). Thus, the complex c formed by the ligand bound to the i -sth PCBS is c^i , and the complex formed by the ligand bound to the catalytic site is called c^* . This change in notation was not incorporated in the schematic in (1b) to show similarity to the MM model. Based on the schematic in Figure 1b and according to the rate law, the change in the concentration of each species can be expressed as:

$$\frac{ds}{dt} = \sum_i k_{-1}^i c^i - \sum_i k_1^i e \cdot s, \tag{1}$$

$$\frac{dc^i}{dt} = k_1^i e \cdot s - k_{-1}^i c^i - k_2^i c^i + k_2^i c^*, \tag{2}$$

$$\frac{dc^*}{dt} = \sum_i k_2^i c^i - \sum_i k_2^i c^* - k_3 c^*, \tag{3}$$

$$\frac{dp}{dt} = k_3 \cdot c^*. \tag{4}$$

Under the assumption that substrate concentration is much larger than enzyme concentration ($s \gg e$), we can work with the steady-state regime approximation of our reaction. In this case, we can then work assuming constant velocities, and we have that the concen-

trations of the enzyme substrate complex at each PCBS (c^i) and at the catalytic site (c^*) do not change. This is expressed as follows:

$$\frac{dc^i}{dt} \cong 0, \quad \frac{dc^*}{dt} \cong 0. \tag{5}$$

Furthermore, we have the following equation, representing the mass balance for the enzyme:

$$e + \sum_i c^i + c^* = E_T, \tag{6}$$

where E_T is the total molar concentration of the enzyme. The following Michaelis–Menten type equation is obtained by solving the system of Equations (2), (3) and (6) after expressing each equation as a function of c^* to replace it in Equation (4).

$$\frac{dp}{dt} = \frac{k_3 \sum_i \frac{Q}{Q_i + Q} E_T s}{\sum_i \frac{1}{Q_i + Q} + s} \tag{7}$$

where Q and Q_i are:

$$Q = \frac{\sum_i \frac{k_1^i k_2^i}{k_{-1}^i + k_2^i}}{\sum_i \frac{k_{-2}^i k_1^i}{k_1^i + k_2^i} + k_3} \tag{8}$$

$$Q_i = \frac{k_1^i}{k_{-1}^i + k_2^i} + \left(\frac{k_{-2}^i}{k_{-1}^i + k_2^i} \right) \left(\frac{\sum_i \frac{k_1^i k_2^i}{k_{-1}^i + k_2^i}}{\sum_i \frac{k_{-2}^i k_1^i}{k_1^i + k_2^i} + k_3} \right) \tag{9}$$

Under these considerations, with a total of i PCBSs (Figure 1b), the enzyme kinetic parameters K_M (11) and V_{max} (10) adopt more complex forms than for the kinetic scheme without PCBSs (Figure 1a). This is analogous to the equation obtained (Appendix A.2) for two PCBSs.

$$V_{max} = k_3 \frac{Q}{\sum_i Q_i + Q} E_T \tag{10}$$

$$K_M = \frac{1}{\sum_i Q_i + Q} \tag{11}$$

If we consider the kinetic constants $k_j^i > 0$ to be fixed, the factors Q and Q_i increase with the number of PCBSs. According to (10) and (11), both V_{max} and K_M decrease asymptotically with the number of PCBSs, to a minimum value that is determined by the values of the kinetic constants. However, the decrease in K_M is sharper than the decrease in V_{max} because the latter is smoothed by the Q factor at the numerator in (10). It is also interesting to note that for this model the *substrate specificity*, which is determined by the ratio $V_{max}/K_M = k_3 E_T Q$ (using (10) and (11)) increases as a function of Q , which increases with the number of PCBSs. As it is proportional to Q , then again we find that, for enzymes with several PCBSs, the experimental determination would give kinetic parameters lower than predicted by the simple model without PCBSs.

For an enzyme with $i = 3$ PCBSs, the kinetic parameters of the enzyme are determined by the following expressions:

$$v_{max} = k_3 \frac{Q}{Q + Q_1 + Q_2 + Q_3} E_T \tag{12}$$

$$K_M = \frac{1}{Q + Q_1 + Q_2 + Q_3} \tag{13}$$

where:

$$Q = \frac{\frac{k_1^1 k_2^1}{k_{-1}^1 + k_2^1} + \frac{k_1^2 k_2^2}{k_{-1}^2 + k_2^2} + \frac{k_1^3 k_2^3}{k_{-1}^3 + k_2^3}}{k_3 + \frac{k_{-2}^1 k_{-1}^1}{k_{-1}^1 + k_2^1} + \frac{k_{-2}^2 k_{-1}^2}{k_{-1}^2 + k_2^2} + \frac{k_{-2}^3 k_{-1}^3}{k_{-1}^3 + k_2^3}} \quad (14)$$

and:

$$Q_1 = \frac{k_1^1}{k_{-1}^1 + k_2^1} + \frac{k_{-2}^1}{k_{-1}^1 + k_2^1} Q \quad (15)$$

$$Q_2 = \frac{k_1^2}{k_{-1}^2 + k_2^2} + \frac{k_{-2}^2}{k_{-1}^2 + k_2^2} Q \quad (16)$$

$$Q_3 = \frac{k_1^3}{k_{-1}^3 + k_2^3} + \frac{k_{-2}^3}{k_{-1}^3 + k_2^3} Q \quad (17)$$

Due to the complexity of the system of equations, a numerical simulation was used to evaluate the relationship between the number of PCBSs and the kinetic parameters.

3.2. Numerical System Simulation with PCBS

To simulate kinetic systems with various PCBSs, we used a Python package that has been used to simulate reactions with various substrates, inhibitors and metabolic pathways for flux control analysis [15]. In our study, we used the “generic reactions” tool of this package to obtain the kinetic parameters of systems with different numbers of PCBSs [16] if equivalent PCBSs with equal binding kinetic constants k_1^i and equal dissociation constants k_2^i are considered. For Table 1, we considered equal PCBSs much more affine than the catalytic site ($k_1^i = k_2^i > k_{cat}^i \gg k_{-1}^i = k_{-2}^i$) to the substrate; on the other hand, for Table 2, we considered PCBSs less affine than the catalytic site ($k_{cat}^i > k_1^i = k_2^i \gg k_{-1}^i = k_{-2}^i$). As we observed when comparing the blue and green curve (Figure 2), for a k_{cat} lower than k_1 and k_2 (blue line), the system reaches a maximum for four PCBSs, unlike the one with a k_{cat} higher than k_1 and k_2 (green line), which does not reach saturation for the number of PCBSs studied. On the kinetic constants k_1 and k_2 , for equal k_{cat} ($k_{cat} = 10$), curves b, c and d (the orange, green and red lines), only the system with $k_1 > k_2$ shows an increase in the catalytic efficiency, mainly for PCBSs=5, overlapping the curves for the other conditions (orange and red line). On the other hand, for a lower k_{cat} ($k_{cat}=1$) than k_1 and k_2 (the purple and brown lines), $k_1 > k_2$ or $k_2 > k_1$ generates similar curves, overlapping in the graph, which shows that for these values of kinetic constants the studied condition ($k_1 > k_2$ or $k_2 > k_1$) is not relevant.

3.3. Dependence of Catalytic Efficiency on PCBS Number

Numerical simulation was used to obtain the product concentration of generic enzyme-catalyzed reactions with and without PCBSs. The values of V_{max} , K_M and the catalytic efficiency were obtained under different values of kinetic constants. As shown in Tables 1–3, under the tested conditions, V_{max} decreases rapidly to a minimum value with an increasing number of PCBSs. For K_M , the same trend is observed but with a sharper decrease with respect to V_{max} . Since the catalytic efficiency is the ratio between K_{cat} and K_M , this parameter is a determinant of substrate selectivity and for comparing enzymes. Our results indicate that this parameter increases with the number of PCBSs for all of the systems studied (Figure 2). As observed in the conditions studied, the values of $k_1, k_2 \geq k_{cat}$ generate a greater increase in catalytic efficiency. If $k_{cat} \geq k_1, k_2$ (b, c and d), the greatest increase in efficiency is obtained with $k_1 > k_2$ (c); furthermore, if $k_1 > k_2$, the system shows the same behavior (b and d).

4. Discussion

Enzymes are amino acid polymers that accelerate chemical reactions by several orders of magnitude under mild environmental conditions. The expression of MM models this

ability well with an equation that is derived from a simple scheme that considers two stages: the first is binding to the catalytic site, and the second is catalysis (Figure 1a). To solve these kinetic equations, we work in a stationary regime and with initial velocities such that the second stage is irreversible. From this expression, the parameters K_M and V_{max} are obtained, which allow for characterizing the properties of an enzyme. However, the MM equation simplifies the first stage by not considering the substrate path from the initial binding site to the catalytic site. According to molecular simulation studies with different systems, the substrate could access the catalytic site by different pathways from several possible PCBs. The number of PCBs or their affinity could determine the enzyme activity, which would explain, for example, the effect on enzyme activity of some mutations far from the catalytic site. Some researchers have already adopted this approach and consider that residues far from the catalytic site may be of interest for designing enzymes with improved properties [17]. Considering this theoretical approach, on the basis of the diagram in Figure 1b, an expression under a steady-state regime of the MM type was obtained for monosubstrate enzymes with different numbers of PCBs. The model establishes a number i of routes of a PCB leading to the catalytic site with reversible steps, which are determined by their kinetic constants. After solving Equations (1)–(4), an undistinguishable expression of the MM equation was obtained, in which the kinetic parameters K_M and V_{max} are determined in complex form by the ratios of kinetic constants Q and Q_i in (8) and (9). Considering the complexity of these expressions, a kinetic parameter neighborhood restricted to $k_1^i = k_2^i$ was explored (Appendix A). Under these restrictions, the catalytic efficiency was increasing with the number of PCBs. If the behavior holds for a larger neighborhood, within the parameters accessible to the model, the overall expression could behave in the same way. For i PCBs, the kinetic parameters decrease as a function of the factors Q and Q_i in (8) and (9), as the number of PCBs increases. According to the obtained equations, the experimental K_M and V_{max} parameters obtained for monosubstrate enzymes with several PCBs correspond to the apparent parameters. This aspect, although real, cannot be appreciated from the experimental data because the model produces the same rectangular hyperbole shape. When analyzing the ratio between k_{cat} and K_M (catalytic efficiency) as a function of the number of PCBs, it is observed that it increases with the number of PCBs; the higher the number of PCBs, the higher the catalytic efficiency. The absence of experimentally measured kinetic constants for the enzymatic reaction steps prevents us from corroborating some of our predictions. However, the K_M and V_{max} parameters are known for mutants in different regions far from the catalytic site and that do not affect the three-dimensional structure [18]. It has been observed that mutations in solvent contact regions of the enzyme β -lactamase, an enzyme that degrades β -lactam antibiotics, do not affect its activity as measured in relation to the sensitivity of the organism to the antibiotic [19]. However, some mutations in the region near the catalytic site can affect activity by making the organism more sensitive to the antibiotic. This effect is evident for some mutants distant to the catalytic site of the β -glycosidase enzyme with altered k_{cat} and K_M parameters [20]. In general, for this enzyme, 10 mutations distant to the catalytic site modify K_M and k_{cat} , thereby decreasing the catalytic efficiency. According to our model, mutations in PCB that decrease or reduce the affinity of these sites for the substrate decrease catalytic efficiency. To explore some neighborhoods of the parameter space, numerical simulations of the kinetic steps were performed, allowing us to obtain the state of the system at each simulated step and the kinetic parameters with the pCBS Kinetics program [16]. As a control for each condition, the kinetic parameters were calculated in the systems with the MM scheme (Figure 1a), obtaining the same value for the simulation and the calculated one. Six conditions of kinetic constants were evaluated, considering different relationships between the constants that determine the formation of the substrate/PCBs complex (k_1^i), constants that determine the passage of the substrate from the PCB to the catalytic site, and the one that directly determines the formation of product (k_{cat} or K_3). For all systems, it is observed that K_M and V_{max} decrease with an increasing number of PCBs (Tables 1–3), and the catalytic efficiency increases. For some conditions, such as a k_{cat} lower

than k_1^i and k_2^i , the increase in the catalytic efficiency is relevant, which could explain the effect of mutations not directly connected to the catalytic site and which can determine the catalytic efficiency.

5. Conclusions

From the studies carried out, an MM-type expression was obtained for a kinetic scheme with several PCBSs, in which the kinetic parameters depend in a complex way on the kinetic constants. By including several PBCSs, the factors Q and Q_i are obtained, which do not exist in the MM model and that make the KM and V_{max} decrease as the number of PCBSs increases. Catalytic efficiency is determined by structural factors that define the (non-stochastic) pathways that the substrate must follow to reach the catalytic site. This is evident by observing that the catalytic efficiency increases linearly with the number of PCBSs up to four PCBSs. Due to the complex expression of Q and Q_i , the dynamic process could determine that some conditions studied are equivalent in spite of the different ratios of the constants. According to the model, it would be interesting to have in vitro studies or simulations to evaluate the predictions and to introduce kinetic constants consistent with an in vitro model.

6. Patents

This section is not mandatory but may be added if there are patents resulting from the work reported in this manuscript.

Author Contributions: Conceptualization, M.I.O. and D.G.S.; methodology, M.P. and O.Y.; software, O.Y.; validation, F.V.-I., D.B. and J.M.P.-D.; formal analysis, M.I.O. and W.T.; investigation, O.Y. and M.I.O.; resources, writing—original draft preparation, M.I.O.; writing—review and editing, J.M.P.-D. and F.G.-N. All authors have read and agreed to the published version of the manuscript.

Funding: This research was funded by the Fondecyt grant 3201013.

Institutional Review Board Statement: Not applicable.

Informed Consent Statement: Not applicable.

Data Availability Statement: The programs generated for this article are available at https://github.com/HumanOsv/pCBS_Kinetics (accessed on 13 October 2023).

Acknowledgments: We acknowledge the Center for Bioinformatics and Integrative Biology and by CenIA (Centro Nacional de Inteligencia Artificial).

Conflicts of Interest: The authors declare no conflict of interest.

Abbreviations

The following abbreviations are used in this manuscript:

MM Michaelis–Menten
PCBS precatalytic binding site

Appendix A

Appendix A.1. Model with Two PCBSs

This section contains the kinetic model for the enzymatic mechanism with two alternative sites of substrate-enzyme binding. Considering the results of the numerical simulation for an enzyme with two PCBSs, we assume that the substrate s binds alternatively to any of two specific sites of the enzyme (e), forming two kinds of enzyme intermediaries (es^1 and es^2); each one is able to transform into a last intermediary (es^*), which forms the product (P) through an elemental kinetic step. Regarding the proposed mechanism (Figure 1b), we deduce a kinetic equation for the initial enzyme activity given by V_0 , defined as the initial rate of product formation

Thus, the rate of the reaction is given by

$$v_0 = \frac{d[p]}{dt} \text{ for } t = 0 \quad (\text{A1})$$

such that there is no initial product and the concentration of the total enzyme (E_T) is much less than the substrate concentration $[E]_T \ll S$

Due to the conservation of the total enzyme,

$$[e] + [es^1] + [es^2] + [es^*] = E_T, \quad (\text{A2})$$

Similar to most enzyme kinetic models, applying the mass action law for each elementary step in the proposed mechanism (Equations (A3)–(A6)):

$$V_0 = [ES^*]K_3 \quad (\text{A3})$$

$$\frac{d[es^1]}{dt} = [E][S]k_1^1 + [ES^*]k_{-2}^1 - [ES](k_{-1}^1 + k_2^1) \quad (\text{A4})$$

$$\frac{d[es^2]}{dt} = [e][s]k_1^2 + [es^*]k_{-2}^2 - [es^1](k_{-1}^2 + k_2^2) \quad (\text{A5})$$

$$\frac{d[es^*]}{dt} = [es^1]k_2^2 + [ES^2]k_2^2 - [ES^*](k_{-2}^1 + k_{-2}^2 + k_3) \quad (\text{A6})$$

where the superscript represents the number of PCBSs, with two for this development. The subscripts represent the number of steps contained in each pathway: two before the catalytic site in the model presented (Figure 1b). Thus, the constant “ k_2^1 ” is the kinetic constant of the second step, from the initial binding site to the catalytic site, for the first PCBS.

In addition, as in the development presented in the results, a steady-state condition is assumed for the concentrations of the enzyme intermediates:

$$\frac{d[es^1]}{dt} = \frac{d[es^2]}{dt} = \frac{d[es^*]}{dt} \approx 0 \quad (\text{A7})$$

Solving Equations (A2)–(A7), the following initial velocity equation for the enzyme is obtained, corresponding to a rectangular hyperbolic graph:

$$v_0 = \frac{[E]_T k_{\text{cat}} [S]}{K_M + [S]} \quad (\text{A8})$$

$$k_{\text{cat}} \equiv \frac{k_1^1 k_2^1 k_3 (k_{-1}^2 + k_2^2) + k_1^2 k_2^2 k_3 (k_{-1}^1 + k_2^1)}{B} \quad (\text{A9})$$

$$K_M \equiv \frac{A}{B} \quad (\text{A10})$$

$$A \equiv k_{-1}^1 k_{-1}^2 (k_{-2}^1 + k_{-2}^2 + k_3) + k_{-1}^2 k_2^1 (k_{-2}^2 + k_3) + k_{-1}^1 k_2^2 (k_{-2}^1 + k_3) + k_2^1 k_2^2 k_3 \quad (\text{A11})$$

$$A \equiv k_{-1}^1 k_{-1}^2 (k_{-2}^1 + k_{-2}^2 + k_3) + k_{-1}^2 k_2^1 (k_{-2}^2 + k_3) + k_{-1}^1 k_2^2 (k_{-2}^1 + k_3) + k_2^1 k_2^2 k_3 \quad (\text{A12})$$

$$B \equiv (B_1 + B_2) \quad (\text{A13})$$

$$B_1 \equiv (k_{-1}^1 k_1^2 + k_1^1 k_{-1}^2) (k_{-2}^1 + k_{-2}^2 + k_3) + k_1^1 k_2^2 (k_{-2}^1 + k_3) \quad (\text{A14})$$

$$B_2 \equiv k_1^2 k_2^1 (k_{-2}^2 + k_3) + k_1^1 k_2^1 (k_{-1}^2 + k_{-2}^2 + k_2^2) + k_1^2 k_2^2 (k_{-1}^1 + k_{-2}^1 + k_2^1) \tag{A15}$$

Equation (A8) is indistinguishable from the equation describing the kinetics for the well-known Michaelis–Menten mechanism, except for the more complex definitions of the kinetic parameters k_{cat} K_M in Equations (A9) and (A10).

Appendix A.2. Model with n PCBSs under Constraints for $k_1^1 = k_1^2$ and $k_{-2}^1 = k_{-2}^2$

This section presents the kinetic model for an extended enzymatic mechanism with n alternative equivalent sites of substrate-enzyme binding.

In the case of $k_1^1 = k_1^2$ and $k_{-2}^1 = k_{-2}^2$, the kinetic mechanism in Figure 1a can be extended to the mechanism of Figure 1b, with n enzyme-substrate complexes $es^{(i)}$ ($i = 1, 2, n$) and kinetic constants independent of i. In this case, assuming $[E]_T \ll S$ and steady-state conditions for the enzyme intermediaries, V_0 (Equation (A1)) is calculated as follows:

$$V_0 = [ES^*]K_3 \tag{A16}$$

$$\frac{d[es^i]}{dt} = [e][s]k_1^i + [es^*]k_{-2}^i - [es](k_{-1}^i + k_2^i) \tag{A17}$$

$$\frac{d[es^*]}{dt} = k_2 \sum_{i=1}^n [es^i] - [es^*](nk_{-2}^i + k_3) \tag{A18}$$

$$\frac{d[es^i]}{dt} = d[es^*]dt \approx 0 \tag{A19}$$

In steady-state conditions:

$$\frac{d[es^{(i)}]}{dt} = \frac{d[es^*]}{dt} \approx 0 \tag{A20}$$

For conservation of the total enzyme:

$$[E]_T = e + es^* + \sum_{i=1}^n es^i \tag{A21}$$

Defining $[es]$ as:

$$[es] \equiv \sum_{i=1}^n [es^i] \tag{A22}$$

and from Equations (A16)–(A22), the following set of equations is obtained:

$$\frac{d[es]}{dt} = [e][s]nk_1 + [es^*]nk_{-2} - [ES](k_{-1} + k_2) \tag{A23}$$

$$\frac{d[es]}{dt} = \frac{d[es^*]}{dt} \approx 0 \tag{A24}$$

$$\frac{d[es^*]}{dt} = k_2[es] - [es] \cdot n \cdot k_{-2} + k_3 \tag{A25}$$

$$[E]_T = e + es^* + es \tag{A26}$$

$$[E]_T = e + es^* + es \tag{A27}$$

From (A1) and (A23)–(A26), V_0 is obtained as in (A8) with the following kinetic parameters:

$$k_{cat} = \frac{k_3}{1 + \frac{nk_{-2} + k_3}{k_2}} \tag{A28}$$

$$K_M = \frac{nk_{-2}k_{-1} + k_3(k_{-1} + k_2)}{nk_1(nk_{-2} + k_2 + k_3)} \tag{A29}$$

Note that the equation system of (A23)–(A27) is the same one that can be derived from the kinetic mechanism in Figure 1a. Therefore, the kinetic mechanisms in Figure 1b have the same kinetics. Moreover, it can be verified that for $n = 2$ in (A28) and (A29), the obtained kinetic parameters are the same ones obtained in Appendix A for $k_{-1}^1 = k_1^2$ and $k_{-2}^1 = k_2^2$ in (A9) and (A10).

Finally, assuming $k_2 \gg nk_{-2} + k_1 + k_3$ in (A28) and (A29), we have

$$k_{cat} \approx k_3 \tag{A30}$$

and

$$K_M \approx \frac{k_3}{nk_1} \tag{A31}$$

Appendix A.3. Algorithm Used

Example for two PCBs

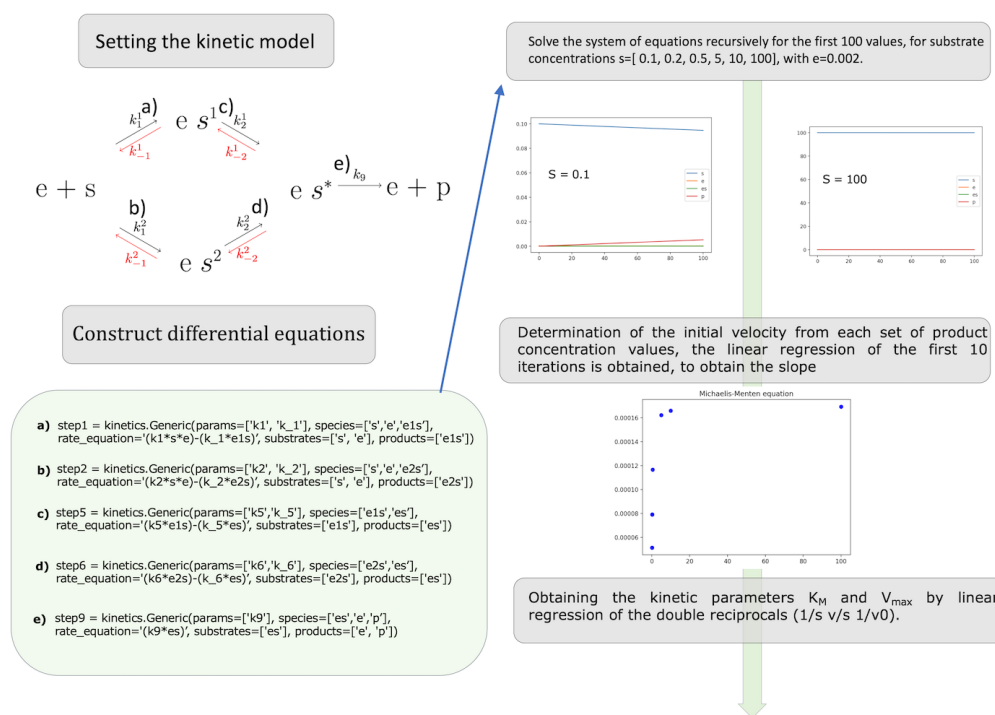


Figure A1. Schematic of the algorithm used for enzyme simulation with various PCBs. This program written in Python is versatile and can be used to represent different reaction schemes based on differential equations using the law of mass action to determine the concentration of each species recursively.

References

1. Ma, X.; Hortelao, A.C.; Patino, T.; Sanchez, S. Enzyme catalysis to power micro/nanomachines. *ACS Nano* **2016**, *10*, 9111–9122. [[CrossRef](#)] [[PubMed](#)]
2. Riziotis, I. Ribeiro, A.J.M. Borkakoti, N. Thornton, J.M. Conformational Variation in Enzyme Catalysis: A Structural Study on Catalytic Residues. *JMB* **2022**, *434*, 167517.
3. Osuna, S. Conformational Variation in Enzyme Catalysis: The challenge of predicting distal active site mutations in computational enzyme design. *Wires Comput. Mol. Sci.* **2021**, *11*, e1502.
4. Marques, S.M.; Bednar, D.; Damborsky, J. Computational study of protein-ligand unbinding for enzyme engineering. *Front. Chem.* **2016**, *10*, 650–665. [[CrossRef](#)]
5. Jagger, B.R.; Kochanek, S.E.; Haldar, S.A.; Rommie, E.; Mulholland, A.J. Multiscale simulation approaches to modeling drug–protein binding. *Curr. Opin. Struct. Biol.* **2020**, *61*, 213–221. [[CrossRef](#)] [[PubMed](#)]
6. Nerukh, D.; Okimoto, N.; Suenaga, A.; Taiji, M. Ligand diffusion on protein surface observed in molecular dynamics simulation. *Curr. Opin. Struct. Biol.* **2012**, *3*, 3476–3479. [[CrossRef](#)] [[PubMed](#)]
7. Ferrario, V.; Fischer, M.; Zhu, Y.; Pleiss, J. Modelling of substrate access and substrate binding to cephalosporin acylases. *J. Phys. Chem. Lett.* **2019**, *9*, 12402. [[CrossRef](#)] [[PubMed](#)]
8. Buch, I.; Giorgino, T.; De Fabritiis, G. Complete reconstruction of an enzyme-inhibitor binding process by molecular dynamics simulations. *Proc. Natl. Acad. Sci. USA* **2011**, *108*, 10184–10189. [[CrossRef](#)]
9. Lorsch, J.R. Chapter One—Practical Steady-State Enzyme Kinetics. In *Laboratory Methods in Enzymology: Protein Part A*; Lorsch, J., Ed.; Academic Press: Baltimore, MD, USA, 2007; pp. 3–15.
10. Voet, D.; Voet, J. Chapter fourteen—Rates of Enzymatic Reactions. In *Biochemistry*; Lorsch, J., Ed.; Academic Press: Baltimore, MD, USA, 2007; pp. 3–15.
11. Goutelle, S.; Maurin, M.; Rougier, F.; Barbaut, X.; Bourguignon, L.; Ducher, M.; Maire, P. The Hill equation: A review of its capabilities in pharmacological modelling. *Fundam. Clin. Pharmacol.* **2008**, *22*, 633–648. [[CrossRef](#)]
12. Burke, M.A. Maini's many contributions to mathematical enzyme kinetics: A review. *J. Theor. Biol.* **2019**, *481*, 24–27. [[CrossRef](#)]
13. Baez, J.C.; Pollard, B.S. A compositional framework for reaction networks. *Rev. Math. Phys.* **2017**, *29*, 1750028. [[CrossRef](#)]
14. Feinberg, M. Nondegeneracy of Semi-open Reaction Networks: An Enzyme Example and the Wnt Pathway. In *Foundations of Chemical Reaction Network Theory*; Springer: Cham, Switzerland, 2019; pp. 3–15.
15. Custom Reactions. Available online: <https://github.com/willfinnigan/kinetics/tree/master/docs> (accessed on 14 August 2023).
16. pCBS Kinetics. Available online: https://github.com/HumanOsv/pCBS_Kinetics (accessed on 14 August 2023).
17. Finnigan, W.; Cutlan, R.; Snajdrova, R.; Adams, J.P.; Littlechild, J.A.; Harmer, N.J. Engineering a seven enzyme biotransformation using mathematical modelling and characterized enzyme parts. *ChemCatChem* **2019**, *11*, 3474–3489. [[CrossRef](#)]
18. Wilding, M.; Hong, N.; Spence, M.; Buckle, A.M.; Jackson, C.J. Protein engineering: the potential of remote mutations. *Biochem. Soc. Trans* **2019**, *47*, 701–711. [[CrossRef](#)] [[PubMed](#)]
19. Jacquier, H.; Birgy, A.; Le Nagard, H.; Mechulam, Y.; Schmitt, E.; Glodt, J.; Bercot, B.; Petit, E.; Poulain, J.; Barnaud, G. Capturing the mutational landscape of the beta-lactamase TEM-1. *Proc. Natl. Acad. Sci. USA* **2013**, *47*, 13067–13072. [[CrossRef](#)] [[PubMed](#)]
20. Mendonça, L.M.F.; Marana, S.R. Single mutations outside the active site affect the substrate specificity in a β -glycosidase. *Biochim. Biophys. Acta Proteins Proteom.* **2011**, *1814*, 13067–13072. [[CrossRef](#)] [[PubMed](#)]

Disclaimer/Publisher's Note: The statements, opinions and data contained in all publications are solely those of the individual author(s) and contributor(s) and not of MDPI and/or the editor(s). MDPI and/or the editor(s) disclaim responsibility for any injury to people or property resulting from any ideas, methods, instructions or products referred to in the content.